iScience, Volume *23*

Supplemental Information

Epigenetic Regulation of Wnt Signaling by Carboxamide-Substituted Benzhydryl Amines that Function as Histone Demethylase Inhibitors

Wen Zhang, Vitaliy M. Sviripa, Yanqi Xie, Tianxin Yu, Meghan G. Haney, Jessica S. Blackburn, Charles A. Adeniran, Chang-Guo Zhan, David S. Watt, and Chunming Liu

Supplemental Information

Epigenetic Regulation of Wnt Signaling by Carboxamide-substituted Benzhydryl Amines That Function as Histone Demethylase Inhibitors

Wen Zhang, Vitaliy M. Sviripa, Yanqi Xie, Tianxin Yu, Meghan G. Haney,

Jessica S. Blackburn, Charles A. Adeniran, Chang-Guo Zhan,

David S. Watt, and Chunming Liu

SUPPLEMENTAL FIGURES

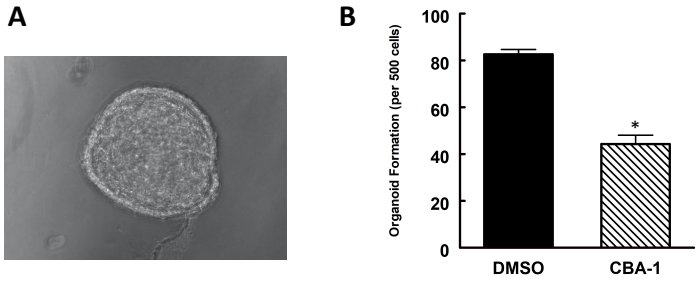

Figure S1. Effects of CBA-1 on colon cancer organoids. Related to Figure 1.

A. Colon cancer organoids from $Apc^{f/+}$/$Kras^{LSL\text{-}G12D}$/Villin-Cre mouse model. **B. CBA-1** (3 μM) inhibited colon cancer organoids formation (* $p < 0.01$; $n = 3$).

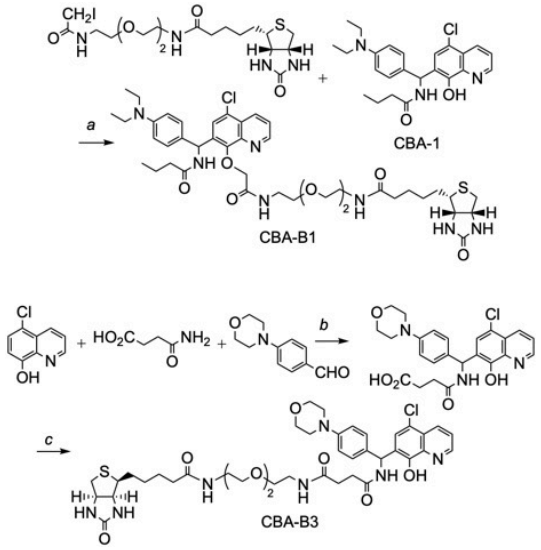

Figure S2. Biotinylated CBAs. Related to Figure 3.

Synthesis of additional biotinylated analogs of **CBA-1**. Synthesis of **CBA-B1**. Legend: *a*, CBA-1 (1 eq), *N*-(2-(2-(2-iodoacetamido)ethoxy)ethyl)-5-((*3aS,4S,6aR*)-2-oxohexahydro-1*H*-thieno[3,4-*d*]imidazol-4-yl)pentanamide (1 eq), K_2CO_3 (1.3 eq), dimethylformamide, 80°C, 3 h (20% yield). Synthesis of **CBA-B2** displayed in **Fig. 3**. Synthesis of **CBA-B3**. Legend: *b*, 5-chloroquinolin-8-ol (1 eq), 4-amino-4-oxobutanoic acid (1 eq), 4-morpholinobenzaldehyde (1.1 eq), 160°C, 50 min followed by dilution with isopropanol to induce precipitation (78% yield); *c*, *N*-(2-(2-(2-aminoethoxy)ethoxy)ethyl)-5-(2-oxohexahydro-1*H*-thieno[3,4-*d*]imidazol-4-yl)pentanamide (2 eq), 1-ethyl-3-(3-dimethylaminopropyl)carbodiimide hydrochloride (2 eq), 1-hydroxybenzotriazole (2 eq), triethylamine (2 eq), 12 h, 25°C (37% yield).

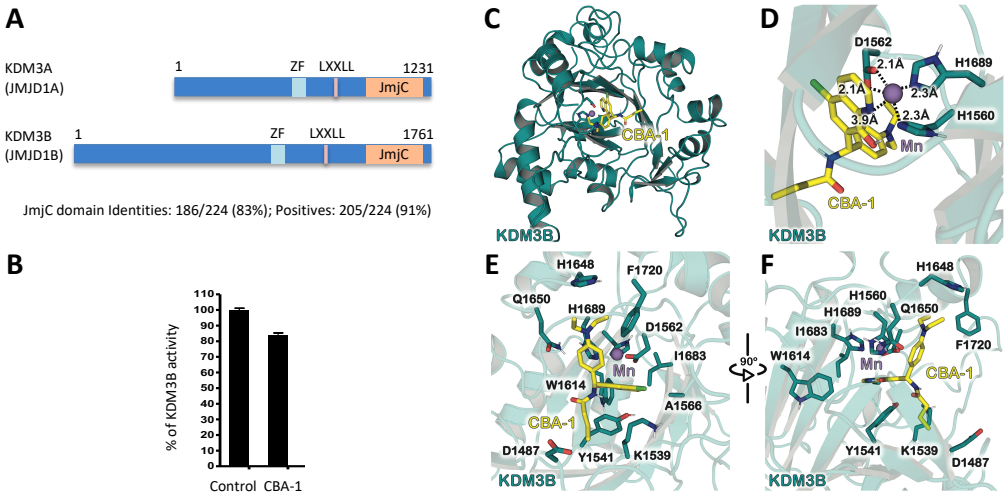

Figure S3. Molecular modeling of the binding site of KDM3B with CBA-1. **Related to Figure 4.**

A. The structures of KDM3A and KDM3B. **B.** Activity of **CBA-1** in KDM3B inhibition. **C.** Global view of the binding of **CBA-1** to KDM3B. Cartoon model representations are shown of the KDM3A in teal. **CBA-1** is shown in stick model and colored yellow. **D**. Local view of the Mn^{2+} binding site including **CBA-1**. Residues involved in the binding site are shown with stick model and colored the same color as its protein backbone. Dashed lines represent the coordination with distances shown close to the respective lines. **E**. Shown here is KDM3B with a focus on the side chain residue interactions between **CBA-1** and residues of KDM3B. **F**. Shown here is **CBA-1** surrounded by residues of KDM3B that are within 3 Å of the inhibitor.

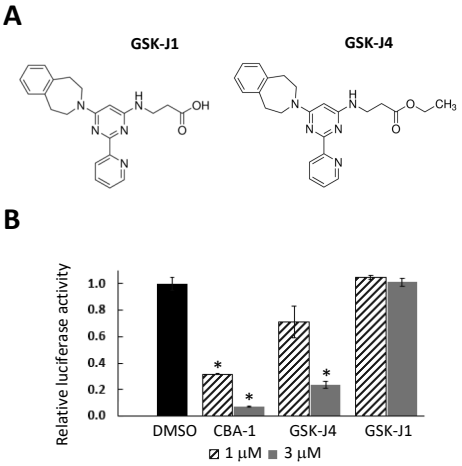

Figure S4. Structures and activities of GSK-J1 and GSKJ4. Related to Figure 4.

A. Structures of GSK-J1 and GSK-J4. **B**. Effects of GSK-J1 and GSK-J4 on Wnt signaling (* $p < 0.0001$; $n = 3$).

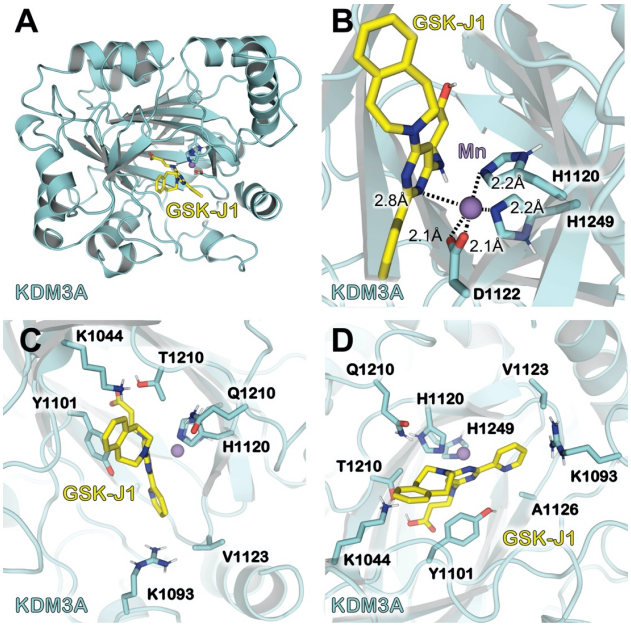

Figure S5. Molecular modeling of the binding site of KDM3A with GSK-J1. Related to Figure 4.

A. Global view of the binding of GSK-J1 to KDM3A. Cartoon representations are shown of the KDM3A in cyan. GSK-J1 is shown in stick model and colored yellow. **B**. Local view of the Mn^{2+} binding site including GSK-J1. Residues involved in the binding site are shown in stick model and colored the same color as its protein backbone. Dashed lines represent the coordination with distances shown. **C**. Shown here is GSK-J1 surrounded by residues of KDM3A that are within 4 Å of the inhibitor. **D**. Shown here is an alternative view of GSK-J1 and the surrounding KDM3A residues.

TRANSPARENT METHODS

Chemistry

Chemicals were purchased from either Millipore Sigma (St. Louis, MO) or Fisher Scientific (Hampton, NH) unless otherwise specified. Solvents were used from commercial vendors without further purification unless otherwise noted. Nuclear magnetic resonance spectra were acquired on a Varian (^{1}H at 400MHz; ^{13}C at 100MHz) instrument. High resolution electrospray ionization (ESI) mass spectra were recorded on an LTQ-Orbitrap Velos mass spectrometer (Thermo Fisher Scientific, Waltham, MA, USA). The FT resolution was set at 100,000 (at 400 *m*/*z*). Samples were introduced through direct infusion using a syringe pump with a flow rate of 5μL/min. Compounds were chromatographed on preparative layer Merck silica gel F254 (Fisher Scientific) plates unless otherwise indicated.

***N*-((5-Chloro-8-hydroxyquinolin-7-yl)(4-(diethylamino)phenyl)methyl)butyramide (CBA-1).** A mixture of 300 mg (1.67 mmol, 1 eq) of 5-chloroquinolin-8-ol, 300 mg (1.67 mmol, 1 eq) of 4-(diethylamino)benzaldehyde, and 580 mg (6.68 mmol, 4 eq) of butyramide was stirred at 130ºC for 2 h. The heating bath was removed, and 3 mL of isopropanol were added to the mixture. The mixture was allowed to cool 25ºC, and a precipitate was collected by filtration to provide 510 mg (71%) of **CBA-1**: mp 195-197°C. ^{1}H NMR (400 MHz, DMSO-d_6) δ 10.16 (s, 1H), 8.94 (dd, J = 4.2, 1.6 Hz, 1H), 8.59 (d, J = 8.6 Hz, 1H), 8.47 (dd, J = 8.5, 1.6 Hz, 1H), 7.73 (s, 1H), 7.7 (dd, J = 8.6, 4.2 Hz, 1H), 7 (d, J = 8.6 Hz, 2H), 6.57 (d, J = 8.7 Hz, 2H), 6.54 (d, J = 8.8 Hz, 1H), 3.27 (q, J = 7 Hz, 4H), 2.18 (t, J = 7.3 Hz, 2H), 1.64-1.45 (m, 2H), 1.03 (t, J = 7 Hz,

6H), 0.86 (t, *J* = 7.4 Hz, 3H). ^{13}C NMR (101 MHz, DMSO-d_6) δ 171.2, 149.05, 148.85, 146.33, 138.62, 132.45, 128.03 (two C), 127.95, 126.51, 126.21, 124.57, 122.71, 118.36, 111.32 (two C), 49.01, 43.61(two C), 37.25, 18.83, 13.63, 12.39 (two C). HRMS (ESI) Calcd for $C_{24}H_{29}ClN_3O_2$ [MH^+]: 426.1943. Found: 426.1946.

***N*-(2-(2-(2-(2-((7-(Butyramido(4-(diethylamino)phenyl)methyl)-5-chloroquinolin-8-yl)oxy)acetamido)ethoxy)ethoxy)ethyl)-5-((*3aR,4R,6aS*)-2-oxohexahydro-1*H*-thieno[3,4-*d*]imidazol-4-yl)pentanamide (CBA-B1)**. To a solution of 51 mg (0.12 mmol) of **CBA-1** in 0.5 mL of N,N-dimethylformamide (DMF) were added 22 mg (0.16 mmol, 1.3 eq) of potassium carbonate. The suspension was stirred for 15 min at 25ºC, and 50 mg (0.12 mmol, 1 eq) of *N*-(2-(2-(2-iodoethoxy)ethoxy)ethyl)-5-(2-oxohexahydro-1*H*-thieno[3,4-*d*]imidazol-4-yl)pentanamide was added. The mixture was stirred at 80ºC for 4 h. After cooling to room temperature, the mixture was poured into water, extracted with dichloromethane, dried over magnesium sulfate and concentrated. The crude product was purified by chromatography using 1:10 methanol-dichloromethane (R_f 0.33) to provide 21 mg (20%) of **CBA-B1**. ^{1}H NMR (400 MHz, $CDCl_3$-*d*) δ 8.95-8.86 (m, 1H), 8.6 (q, *J* = 13.2, 6.2 Hz, 1H), 8.54 (dd, *J* = 8.6, 1.7 Hz, 1H), 7.64 (d, *J* = 2.1 Hz, 1H), 7.52 (ddd, *J* = 8.5, 4.2, 1.4 Hz, 1H), 7.05 (d, *J* = 8.7 Hz, 2H), 6.58 (d, *J* = 8.8 Hz, 2H), 6.54 (d, *J* = 6.8 Hz, 1H), 6.45 (t, *J* = 6.4 Hz, 1H), 5.78 (s, 1H), 5.74 (s, 1H), 4.94 (d, *J* = 6.6 Hz, 1H), 4.82 (dd, *J* = 14.6, 5.9 Hz, 1H), 4.47-4.38 (m, 2H), 4.27-4.19 (m, 1H), 3.72-3.63 (m, 4H), 3.63-3.57 (m, 4H), 3.5 (t, *J* = 5.1 Hz, 2H), 3.4-3.26 (m, 6H), 3.14-3.03 (m, 1H), 2.86 (dd, *J* = 12.8 and 5 Hz, 1H), 2.67 (dd, *J* = 12.8, 4.4 Hz, 1H), 2.29-2.22 (m, 2H), 2.15-2.07 (m, 2H), 1.71-1.64 (m, 3H), 1.63-1.53 (m, 3H), 1.45-1.32 (m, 2H), 1.12 (t, *J* = 7 Hz, 6H), 0.96 (t, *J* = 7.4 Hz, 3H). ^{13}C NMR (101 MHz, $CDCl_3$) δ 173.26, 172.57, 169.82, 163.37, 150.6, 150.26, 147.58,

143, 135.31, 135.29, 133.61, 128.61, 126.93, 126.8, 126.18, 125.74, 122.18, 111.89, 77.36, 73.88, 70.44, 70.33, 70, 61.87, 60.19, 55.4, 52.29, 44.47, 40.64, 39.26, 39.12, 38.64, 35.83, 28.14, 25.56, 19.31, 13.99, 12.66. HRMS (ESI) Calcd for $C_{42}H_{59}ClN_7O_7S$ [MH^+]: 840.3880. Found: 840.3876.

1-(4-(Butyramido(5-chloro-8-hydroxyquinolin-7-yl)methyl)phenyl)-*N*-(2-(2-(2-(5-((*3aS,4S,6aR*)-2-oxohexahydro-1*H*-thieno[3,4-*d*]imidazol-4-yl)pentanamido)ethoxy)-ethoxy)ethyl)piperidine-4-carboxamide (CBA-B2). To a stirred solution of 120 mg (0.53 mmol) of 1-(4-formylphenyl)piperidine-4-carboxylic acid in 2 ml of DMF was added successively 100 mg (0.80 mmol, 1.5 eq) of 1-hydroxybenzotriazole (HOBt), 150 mg (0.8 mmol, 1.5 eq) of *N*-(3-dimethylaminopropyl)-*N'*-ethylcarbodiimide hydrochloride, 200 mg (0.53 mmol, 1 eq) of *N*-(2-(2-(2-aminoethoxy)ethoxy)ethyl)-5-(2-oxohexahydro-1*H*-thieno[3,4-*d*]imidazol-4-yl)pentanamide and 54 mg (0.8 mmol, 1.5 eq) of triethylamine. The mixture was stirred for 12 h at 25ºC, poured in brine, extracted with dichloromethane, dried over magnesium sulfate and concentrated. The crude product was purified by chromatography using 1:10 methanol-dichloromethane (R_f 0.18) to provide 180 mg (57%) of 1-(4-formylphenyl)-*N*-(2-(2-(2-(5-(2-oxohexahydro-1*H*-thieno[3,4-*d*]imidazol-4-yl)pentanamido)ethoxy)ethoxy)ethyl)-piperidine-4-carboxamide. A mixture of 110 mg (0.19 mmol) of this aforementioned carboxamide, 33 mg (0.19 mmol, 1 eq) of 5-chloroquinolin-8-ol, and 97 mg (1.12 mmol, 6 eq) of butyramide was stirred at 150ºC for 2 h. The heating bath was removed, and 2 mL of methanol were added to the mixture. The mixture was allowed to cool 25ºC, and a precipitate was collected by filtration. The precipitate was purified by chromatography using 1:10 methanol-dichloromethane (R_f 0.2) to provide 180 mg (57%) of **CBA-B2**. ^{1}H NMR (400 MHz, DMSO-d_6) δ 10.21 (s, 1H), 8.95 (d, *J* =

3.1 Hz, 1H), 8.64 (d, *J* = 8.7 Hz, 1H), 8.48 (d, *J* = 8.5 Hz, 1H), 7.83 (q, *J* = 6.1 Hz, 2H), 7.74-7.69 (m, 1H), 7.06 (d, *J* = 8.6 Hz, 2H), 6.86 (d, *J* = 8.5 Hz, 2H), 6.59 (d, *J* = 8.7 Hz, 1H), 6.4 (s, 1H), 6.34 (s, 1H), 4.38-4.23 (m, 1H), 4.17-4.06 (m, 1H), 3.65 (d, *J* = 12.3 Hz, 2H), 3.54-3.47 (m, 4H), 3.43-3.36 (m, 4H), 3.22-3.14 (m, 4H), 3.13-3.03 (m, 1H), 2.8 (dd, *J* = 12.4, 5 Hz, 1H), 2.66-2.53 (m, 3H), 2.31-2.21 (m, 1H), 2.18 (t, *J* = 7.3 Hz, 2H), 2.06 (t, *J* = 7.4 Hz, 2H), 1.78-1.38 (m, 11H), 1.34-1.2 (m, 2H), 0.86 (t, *J* = 7.4 Hz, 3H). ^{13}C NMR (101 MHz, DMSO-d_6) δ 174.31, 172.1, 171.27, 162.67, 150.01, 149.1, 148.95, 138.62, 132.47, 131.68, 127.66, 126.21, 126.13, 124.64, 122.79, 118.42, 115.64, 69.52, 69.14, 69.05, 61.02, 59.17, 55.4, 48.96, 48.38, 41.69, 38.42, 37.24, 35.09, 28.18, 28.02, 27.96, 25.25, 18.81, 13.61. HRMS (ESI) Calcd for $C_{42}H_{57}ClN_7O_7S$ [MH^+]: 838.3723. Found: 838.3730.

***N*^{1}-((5-Chloro-8-hydroxyquinolin-7-yl)(4-morpholinophenyl)methyl)-*N*^{4}-((2-(2-(5-((*3aS,4S,6aR*)-2-oxohexahydro-1*H*-thieno[3,4-*d*]imidazol-4-yl)pentanamido)-ethoxy)ethoxy)methyl)succinamide (CBA-B3).** A mixture of 300 mg (1.67 mmol) of 5-chloroquinolin-8-ol, 350 mg (1.84 mmol, 1.1 eq) of 4-morpholinobenzaldehyde, and 200 mg (1.67 mmol, 1 eq) of succinamic acid was stirred at 160ºC for 1 h. The heating bath was removed, and 3 mL of isopropanol were added to the mixture. The mixture was cooled to 25˚C, and a precipitate was collected by filtration to provide 380 mg (48%) of crude 4-(((5-chloro-8-hydroxyquinolin-7-yl)(4-morpholinophenyl)methyl)amino)-4-oxobutanoic acid. To a stirred solution of 63 mg (0.13 mmol) of this crude product in 1 mL of DMF were successively added 36 mg (0.27 mmol, 2 eq) of 1-hydroxybenzotriazole (HOBt), 51 mg (0.27 mmol, 2 eq) of *N*-(3-dimethylaminopropyl)-*N*′-ethylcarbodiimide hydrochloride, 50 mg (0.13 mmol, 1 eq) of *N*-(2-(2-(2-aminoethoxy)ethoxy)ethyl)-5-(2-oxohexahydro-1*H*-thieno[3,4-*d*]imidazol-4-yl)pentanamide

and 37 mL (0.27 mmol, 2 eq) of triethylamine. The mixture was stirred for 12 h at 25ºC and poured into water. A precipitate was collected by filtration to provide 41 mg (37%) of pure **CBA-B3**. ^{1}H NMR (400 MHz, DMSO-d_6) δ 10.19 (s, 1H), 8.91 (dd, J = 4.2, 1.6 Hz, 1H), 8.68 (d, J = 8.7 Hz, 1H), 8.44 (dd, J = 8.6, 1.6 Hz, 1H), 7.84 (t, J = 5.6 Hz, 1H), 7.79 (t, J = 5.7 Hz, 1H), 7.7-7.63 (m, 1H), 7.07 (d, J = 8.7 Hz, 2H), 6.83 (d, J = 8.8 Hz, 2H), 6.56 (d, J = 8.7 Hz, 1H), 6.37 (s, 1H), 6.31 (s, 1H), 4.31-4.22 (m, 1H), 4.15-4.04 (m, 1H), 3.69-3.63 (m, 4H), 3.44 (s, 4H), 3.38-3.31 (m, 4H), 3.14 (q, J = 5.9 Hz, 4H), 3.08-3.03 (m, 2H), 3.03-2.98 (m, 4H), 2.77 (dd, J = 12.4, 5.1 Hz, 1H), 2.53 (d, J = 12.5 Hz, 1H), 2.44-2.38 (m, 2H), 2.31 (d, J = 6.9 Hz, 2H), 2.02 (t, J = 7.4 Hz, 2H), 1.63-1.5 (m, 1H), 1.51-1.35 (m, 3H), 1.32-1.18 (m, 2H). ^{13}C NMR (101 MHz, DMSO-d_6) δ 172.12, 171.37, 170.65, 162.68, 150.01, 149.1, 148.89, 138.62, 132.48, 127.6, 126.24, 126.06, 124.68, 122.81, 118.52, 115.02, 69.5, 69.15, 69.09, 66.04, 61.02, 59.18, 55.41, 48.96, 48.55, 39.83, 38.54, 38.43, 35.09, 30.76, 30.67, 28.18, 28.03, 25.25. HRMS (ESI) Calcd for $C_{40}H_{53}ClN_7O_8S$ [MH^+]: 826.3359. Found: 826.3357.

Biology

Drug screening. Stable HEK293T cell line transfected with a TOPFlash plasmid was treated with DMSO or 2.5 μM of each compound. After 6 h, the cells were treated with 25 mM LiCl to activate Wnt signaling. The inhibition ratios of these compounds were determined. The leading compounds were validated at 500 nM. The compound library was from University of Cincinnati Drug Discovery Center.

Cell culture. LS174T colon cancer cells were cultured in EMEM (ATCC, 30-2003) containing 10% Fetal Bovine Serum (Sigma F0926). HEK293T and the DLD-1 and SW620 colon cancer cells were cultured in DMEM (Sigma D6429) containing 10% Fetal Bovine Serum (Sigma, F0926). For proliferation assays, cells ($3.5x10^4$ cells per well) were split into 12-well plates. After 24 h, 1 μl of each compound was added to each well. DMSO was used as a control. Each experiment was done in triplicate. Cell viability and number were analyzed using the Vi-Cell XR Cell Viability Analyzer (Beckman Coulter). ShRNA construct for KDM3A was ordered from Sigma. HEK293T cells were transfected with lentivirus packaging plasmids psPAX2 and pMD2.G, as well as control shRNA plasmids. Lentivirus stock was collected 48h after transfection. Cells were infected by the lentivirus stock for 12h, followed by sustained growth in fresh medium for 36-48h. Infected cell lines were seeded in 12-well plate for proliferation assay. ShRNA efficiency was tested by Western blotting using lysates from HEK293T or colon cancer cells transfected with shRNAs. Wnt reporter assay has been described previously(Shi et al., 2015, Zhang et al., 2019).

Biochemistry. Western blotting: Cells were lysed in the appropriate volume of lysis buffer (50 mM HEPES, 100 mM NaCl, 2 mM EDTA, 1% glycerol, 50 mM NaF, 1 mM Na_3VO_4, 1% Triton X-100, with protease inhibitors). KDM3A and KDM3B inhibition assays were performed through the service of BPS Bioscience (San Diego, CA). Antibodies for Wnt target genes, such as Axin2, c-Myc, survivin, cyclin B1 and cyclin D1 have been described previously(Shi et al., 2015, Zhang et al., 2011). KDM3A antibody was purchased from GeneTex (GTX129046). Histone methylation antibodies were purchased from Cell Signaling Technology. To validate the **CBA-1** target, HEK293T cell lysates were incubated with streptavidin beads and biotinylated

CBA-B2 at 4ºC overnight. The beads were washed 3 times with cell lysis buffer and the binding proteins were analyzed by Western blot as previously described(Zhang et al., 2013). Chromatin immunoprecipitation (ChIP) assay was performed with Di-Methyl-Histone H3 (Lys9) antibody (#4658) from Cell Signaling Technology using the method previously described(Evans et al., 2007). The Western blot images were scanned using CanoScan 5600F and the densitometry was analyzed using Adobe photoshop 2020. Real-time qPCR was perform using QuantStudio 3 from Applied Biosystems.

Colon Cancer Organoids. The colon cancer organoids were provided by Professor Tianyan Gao at Markey Cancer Center, University of Kentucky. The organoids were isolated from $Apc^{f/+}$/$Kras^{LSL\text{-}G12D}$/Villin-Cre mouse model(Wen et al., 2017). For 48-well drug screening, the Matrigel containing organoids was digested by 300 µl dispase. The gel was removed by 1000 x 5min spinning. The organoids were digested into single cells by 1 ml Trypsin and washed with 10 ml Advanced DMEM/F12. For each well, 80 µl Matrigel was added to the bottom and 500 cells in 60 µl Matrigel were added to the top. The cells were culture in 250 µl 3D complete medium (Advanced DMEM/F12 supplemented with 1 x N-2, 1 x B-27, 1 mmol/l N-acetylcysteine and 1% penicillin/streptomycin). The cells were treated with DMSO or testing compounds and organoids formation were analyzed using microscope.

Zebrafish Studies. Use and handling of Zebrafish was approved by the University of Kentucky's Institutional Animal Care and Use Committee (IACUC), protocol 2015-2225. For eye phenotype studies, CG1 syngeneic Zebrafish were dechorionated using 1 mg/mL Pronase and treated at 6 hours post-fertilization (hpf) with DMSO, or 1 µM Bio (Millipore Sigma,

B1686-5MG) with or without varying concentrations of **CBA-1** in 200 µL E3 media in 96-well plates. Eye development was assessed after 2 days of treatment. 6xTCF/LEF-miniP:eGFP sheer transgenic Zebrafish (a kind gift from Dave Langenau, Harvard University, Boston, MA) were utilized to assess Wnt signaling *in vivo*. Zebrafish were dechorionated as above at 24 hpf and treated with DMSO, Bio, or **CBA-1** in a 96-well plate in 200 µL E3 media volume. Zebrafish were imaged after 48 hours of treatment. For tail amputation studies, adult 6xTCF/LEF-miniP:eGFP sheer transgenic Zebrafish were anesthetized with Tricaine (Pentair, TRS1) and a single cut was made with a razor blade perpendicular to the fin rays. Fish were allowed to recover for 20 minutes before randomly dividing the fish into treatment groups. Fish were kept in DMSO, 1 µM Bio, or 5 µM **CBA-1** in 250 mL of fish system water for 5 days post-amputation. Drug was changed daily, and the fish were fed on day 2 post-amputation prior to drug change. Fish were imaged and tail growth was assessed at 4 days post-amputation.

Molecular Modeling. Molecular modeling was conducted to determine the KDM3A structure using the KDM3B structure as a template. The KDM3B structure was obtained from a 2.18 Å X-ray crystal structure with RCSB Protein Data Bank (PDB) ID 4C8D. Modeller(Webb and Sali, 2016) was used to build the KDM3A structure and add missing residues to the protein. The homology modeled structure of KDM3A was then energy minimized with 4,000 steps of the deepest decent energy-minimization and 4,000 steps of the conjugate gradient energy-minimization by using the Sander module of the Amber18 package(Case et al., 2018).

Molecular Docking. Molecular docking was conducted to determine the binding poses of inhibitors **CBA-1** and GSK-J1 within the JmjC domain of KDM3A or KDM3B. Gold docking

program(Verdonk et al., 2004, Verdonk et al., 2003) was used to carry out the docking at the metal ion binding site. All structures were imported into the LEaP module of the Amber18(Case et al., 2018) suite of programs(Case et al., 2005) to add hydrogens using the ff14SB(Hornak et al., 2006, Maier et al., 2015) modified version of the Cornell et al.(Cornell et al., 1995) force field. These structures were optimized with 4,000 steps of the deepest decent energy-minimization and 4,000 steps of the conjugate gradient energy-minimization by using the Sander module of the Amber18 package. This series of optimized minimization steps were carried out by applying a harmonic constraint only on the protein and gradually reducing the force constant from 300, 200, 100, 75, 50, and 25 kcal/mol/Å^2. A final minimization step was carried out without applying any harmonic constraint. The figures showing the structures were generated using the PyMol software.(Schrodinger, 2015)

Statistics. Cell proliferation, Western blot, report assay and real-time PCR were performed in triplicates. Microarray and patient clinical data from colon cancer studies were downloaded from the TCGA and GTEx databases. A two-sample t-test was used to compare KDM3A expression in colon adenocarcinoma patients versus normal controls using GEPIA program.[25]

Table S1. Key Resources. Related to all Figures.

REAGENT or RESOURCE	SOURCE	IDENTIFIER
Antibodies		
Rabbit monoclonal anti-c-Myc (N-term)	Abcam	Cat# 1472-1, RRID:AB_562270
Rabbit monoclonal anti-Axin2 (76G6)	Cell Signaling Technology	Cat# 2151, RRID:AB_2062432
Rabbit monoclonal anti-Cyclin d1	Abcam	Cat# 2261-1, RRID:AB_991714
Mouse monoclonal anti-Cyclin B1 (V152)	Cell Signaling Technology	Cat# 4135, RRID:AB_2233956
Rabbit monoclonal anti-Survivin (71G4B7)	Cell Signaling Technology	Cat# 2808, RRID:AB_2063948
Mouse monoclonal anti-beta-Actin	Sigma-Aldrich	Cat# A1978, RRID:AB_476692
Rabbit monoclonal anti-Tri-Methyl-Histone H3 (Lys9) (D4W1U)	Cell Signaling Technology	Cat# 13969, RRID:AB_2798355
Rabbit monoclonal anti-Di-Methyl-Histone H3 (Lys9) (D85B4)	Cell Signaling Technology	Cat# 4658, RRID:AB_10544405
Rabbit monoclonal anti-Di-Methyl-Histone H3 (Lys4) (C64G9)	Cell Signaling Technology	Cat# 9725, RRID:AB_10205451
Rabbit polyclonal anti-Histone H3	Abcam	Cat# ab1791, RRID:AB_302613
Mouse monoclonal anti-GAPDH (GT239)	GeneTex	Cat# GTX627408, RRID:AB_11174761
Rabbit polyclonal anti-KDM3A	GeneTex	Cat# GTX129046
Goat Anti-Rabbit IgG, H & L Chain Specific Peroxidase Conjugate	Millipore	Cat# 401315, RRID:AB_2617117
Goat Anti-Mouse IgG, H & L Chain Specific Peroxidase Conjugate	Millipore	Cat# 401215, RRID:AB_10682749
Bacterial and Virus Strains		
N/A		
Biological Samples		
N/A		
Chemicals, Peptides, and Recombinant Proteins		
XAV939	Sigma-Aldrich	Cat# X3004-5MG; CAS: 284028-89-3
LiCl	Sigma-Aldrich	Cat# L4408-100G; CAS: 7447-41-8
Dimethyl sulfoxide	Sigma-Aldrich	Cat# D2650-100ML; CAS: 67-68-5
Strep-Tactin Superflow Agarose	Millipore	Cat# 71592-3
BIO	Sigma-Aldrich	Cat# B1686; CAS: 667463-62-9
GSK-J1 (sodium salt)	Cayman Chemical	Cat# 12054; CAS: 1797832-71-3
GSK-J4 (hydrochloride)	Cayman Chemical	Cat# 12073; CAS: 1797983-09-5
Critical Commercial Assays		
Dual-Luciferase Reporter Assay System	Promega	Cat# 1910
Vi-Cell XR Reagent Pack for Cell viability analyzer	BECKMAN	Cat# 383260
JMJD1A Homogeneous Assay Kit	BPS Bioscience	Cat# 50412

Deposited Data		
N/A		
Experimental Models: Cell Lines		
Human: 293T Cells	ATCC	Cat# CRL-3216; RRID:CVCL_0063
Human: LS174T Cells	ATCC	Cat# CL-188; RRID:CVCL_1384
Human: SW620 Cells	ATCC	Cat# CCL-227; RRID:CVCL_0547
Human: DLD-1 Cells	ATCC	Cat# CCL-221; RRID:CVCL_0248
Mouse: L Wnt-3A Cells	ATCC	Cat# CRL-2647; RRID:CVCL_0635
Experimental Models: Organisms/Strains		
6xTCF/LEF-miniP:eGFP sheer transgenic Zebrafish	Kind gift from Dave Langenau at Harvard University	N/A
Mouse colon cancer organoids from $Apc^{f/+}/Kras^{LSL-G12D}$/Villin-Cre mouse model	Kind gift from Tianyan Gao at University of Kentucky	N/A
Oligonucleotides		
C-Myc ChIP Primers: Forward: GTGAATACACGTTTGCGGGTTAC; Reverse: AGAGACCCTTGTGAAAAAAACCG	This paper	N/A
Cyclin B1 ChIP primers: Forward: TCTTGCCCGGCTAACCTTTCCAGG; Reverse: TTCCGCCGCAGCACGCCGAGAAGA	This paper	N/A
GAPDH ChIP primers: Forward: CATGTTCGTCATGGGGTGAACCA; Reverse: AGTGATGGCATGGACTGTGGTCAT	This paper	N/A
Recombinant DNA		
pLKO human KDM3A shRNA	Sigma-Aldrich	TRCN0000329990
Software and Algorithms		
Graphpad Prism 5	Graphpad	RRID:SCR_002798 http://www.graphpad.com
GEPIA	Peking University	RRID:SCR_018294 http://gepia.cancer-pku.cn
GOLD	CCDC	RRID:SCR_000188 http:/www.ccdc.cam.ac.uk/Solutions/GoldSuite/Pages/GOLD.aspx
MODELLER	Ben Webb	RRID:SCR_008395 http://salilab.org/modeller/modeller.html
Other		

SUPPLEMENTAL REFERENCES

CASE, D. A., BEN-SHALOM, I. Y., BROZELL, S. R., CERUTTI, D. S., CHEATHAM III, T. E., CRUZEIRO, V. W. D., DARDEN, T. A., DUKE, R. E., GHOREISHI, D., GILSON, M. K., GOHLKE, H., GOETZ, A. W., GREENE, D., HARRIS, R., HOMEYER, N., IZADI, S., KOVALENKO, A., KURTZMAN, T., LEE, T. S., LEGRAND, S., LI, P., LIN, C., LIU, J., LUCHKO, T., LUO, R., MERMELSTEIN, D. J., MERZ, K. M., MIAO, Y., MONARD, G., NGUYEN, C., NGUYEN, H., OMELYAN, I., ONUFRIEV, A., PAN, F., QI, R., ROE, D. R., ROITBERG, A., SAGUI, C., SCHOTT-VERDUGO, S., SHEN, J., SIMMERLING, C. L., SMITH, J., SALOMON-FERRER, R., SWAILS, J., WALKER, R. C., WANG, J., WEI, H., WOLF, R. M., WU, X., XIAO, L., YORK, D. M. & KOLLMAN, P. A. 2018. *AMBER 2018,* University of California, San Francisco.

CASE, D. A., CHEATHAM, T. E., DARDEN, T., GOHLKE, H., LUO, R., MERZ, K. M., ONUFRIEV, A., SIMMERLING, C., WANG, B. & WOODS, R. J. 2005. The Amber biomolecular simulation programs. *Journal of Computational Chemistry,* 26**,** 1668-1688.

CORNELL, W. D., CIEPLAK, P., BAYLY, C. I., GOULD, I. R., MERZ, K. M., FERGUSON, D. M., SPELLMEYER, D. C., FOX, T., CALDWELL, J. W. & KOLLMAN, P. A. 1995. A 2ND GENERATION FORCE-FIELD FOR THE SIMULATION OF PROTEINS, NUCLEIC-ACIDS, AND ORGANIC-MOLECULES. *Journal of the American Chemical Society,* 117**,** 5179-5197.

EVANS, P. M., ZHANG, W., CHEN, X., YANG, J., BHAKAT, K. K. & LIU, C. 2007. Kruppel-like factor 4 is acetylated by p300 and regulates gene transcription via modulation of histone acetylation. *J Biol Chem,* 282**,** 33994-4002.

HORNAK, V., ABEL, R., OKUR, A., STROCKBINE, B., ROITBERG, A. & SIMMERLING, C. 2006. Comparison of multiple amber force fields and development of improved protein backbone parameters. *Proteins-Structure Function and Bioinformatics,* 65**,** 712-725.

MAIER, J. A., MARTINEZ, C., KASAVAJHALA, K., WICKSTROM, L., HAUSER, K. E. & SIMMERLING, C. 2015. ff14SB: Improving the Accuracy of Protein Side Chain and Backbone Parameters from ff99SB. *Journal of Chemical Theory and Computation,* 11**,** 3696-3713.

SCHRODINGER, L. 2015. The PyMOL Molecular Graphics System, Version 1.8.

SHI, J., LIU, Y., XU, X., ZHANG, W., YU, T., JIA, J. & LIU, C. 2015. Deubiquitinase USP47/UBP64E Regulates beta-Catenin Ubiquitination and Degradation and Plays a Positive Role in Wnt Signaling. *Mol Cell Biol,* 35**,** 3301-11.

VERDONK, M. L., BERDINI, V., HARTSHORN, M. J., MOOIJ, W. T. M., MURRAY, C. W., TAYLOR, R. D. & WATSON, P. 2004. Virtual Screening Using Protein−Ligand Docking: Avoiding Artificial Enrichment. *Journal of Chemical Information and Computer Sciences,* 44**,** 793-806.

VERDONK, M. L., COLE, J. C., HARTSHORN, M. J., MURRAY, C. W. & TAYLOR, R. D. 2003. Improved protein–ligand docking using GOLD. *Proteins: Structure, Function, and Bioinformatics,* 52**,** 609-623.

WEBB, B. & SALI, A. 2016. Comparative Protein Structure Modeling Using MODELLER. *Curr Protoc Bioinformatics,* 54**,** 5.6.1-5.6.37.

WEN, Y. A., XING, X., HARRIS, J. W., ZAYTSEVA, Y. Y., MITOV, M. I., NAPIER, D. L., WEISS, H. L., MARK EVERS, B. & GAO, T. 2017. Adipocytes activate mitochondrial fatty acid oxidation and autophagy to promote tumor growth in colon cancer. *Cell Death Dis,* 8**,** e2593.

ZHANG, W., SVIRIPA, V., CHEN, X., SHI, J., YU, T., HAMZA, A., WARD, N. D., KRIL, L. M., VANDER KOOI, C. W., ZHAN, C. G., EVERS, B. M., WATT, D. S. & LIU, C. 2013. Fluorinated N,N-dialkylaminostilbenes repress colon cancer by targeting methionine S-adenosyltransferase 2A. *ACS Chem Biol,* 8**,** 796-803.

ZHANG, W., SVIRIPA, V., KRIL, L. M., CHEN, X., YU, T., SHI, J., RYCHAHOU, P., EVERS, B. M., WATT, D. S. & LIU, C. 2011. Fluorinated N,N-dialkylaminostilbenes for Wnt pathway inhibition and colon cancer repression. *J Med Chem,* 54**,** 1288-97.

ZHANG, W., SVIRIPA, V. M., KRIL, L. M., YU, T., XIE, Y., HUBBARD, W. B., SULLIVAN, P. G., CHEN, X., ZHAN, C. G., YANG-HARTWICH, Y., EVERS, B. M., SPEAR, B. T., GEDALY, R., WATT, D. S. & LIU, C. 2019. An Underlying Mechanism of Dual Wnt Inhibition and AMPK Activation: Mitochondrial Uncouplers Masquerading as Wnt Inhibitors. *J Med Chem,* 62**,** 11348-11358.